ORIGINAL RESEARCH

Preparation and characterization of an iron oxide-hydroxyapatite nanocomposite for potential bone cancer therapy

Murugesan Sneha
Nachiappan
Meenakshi Sundaram

Department of Biomedical Engineering, PSG College of Technology, Tamil Nadu, India

Abstract: Recently, multifunctional magnetic nanostructures have been found to have potential applications in biomedical and tissue engineering. Iron oxide nanoparticles are biocompatible and have distinctive magnetic properties that allow their use in vivo for drug delivery and hyperthermia, and as T_2 contrast agents for magnetic resonance imaging. Hydroxyapatite is used frequently due to its well-known biocompatibility, bioactivity, and lack of toxicity, so a combination of iron oxide and hydroxyapatite materials could be useful because hydroxyapatite has better bone-bonding ability. In this study, we prepared nanocomposites of iron oxide and hydroxyapatite and analyzed their physicochemical properties. The results suggest that these composites have superparamagnetic as well as biocompatible properties. This type of material architecture would be well suited for bone cancer therapy and other biomedical applications.

Keywords: iron oxide, hydroxyapatite, nanocomposite, superparamagnetic, bone cancer

Introduction

Cancer is the most dreaded disease, along with heart disease. Hyperthermia has attracted much interest in the treatment of cancer due to its advantages over chemotherapy and radiotherapy. Using hyperthermia, cancer cells are killed directly within a short period of time, whereas normal cells are unaffected.[1] Magnetic hyperthermia is practiced by applying an external alternating magnetic field which in turn oscillates the magnetic moment of each particle, converting magnetic energy into heat. Superparamagnetic materials for magnetic hyperthermia are promising candidates for antitumor therapy because they have the capacity to destroy deep tumors and are controlled by an external magnetic field.[2] Magnetic nanoparticles have attractive features that could be used effectively in nanomedicine. First, they have a controllable particle size (from a few nanometers to tens of nanometers). Second, they are magnetic, so can be manipulated by an external magnetic field. Third, they can be made to heat up, so can be used as hyperthermia agents, delivering large amounts of thermal energy to tumor cells and destroying them.[3] If an iron oxide nanoparticle is below 45 nm in size, it is classified as superparamagnetic due to its line-type hysteresis loop iron oxide nanoparticles. The magnetite (Fe_3O_4) phase of superparamagnetic iron oxide nanoparticles has numerous in vivo applications, since it can respond to an external stimulus and heat up, and does not retain any magnetism after removal of the external magnetic field.[4,5] Materials that are compatible with bone tissue are preferred for bone repair and hard tissue engineering.[6] Hydroxyapatite (HAp) is widely used in this setting because of its exceptional biocompatibility, bioactivity, and osteoconductivity.[7] A number of

Correspondence: Nachiappan
Meenakshi Sundaram
Department of Biomedical Engineering,
PSG College of Technology,
Coimbatore-04, Tamil Nadu, India
Tel +91 42 2257 2177
Email nms@bme.psgtech.ac.in

Video abstract

Point your SmartPhone at the code above. If you have a QR code reader the video abstract will appear. Or use:
http://youtu.be/rRFw0_DBkBU

researchers have developed a variety of HAp-based magnetic materials for hyperthermia-based treatment of cancer.[8–11]

Murakami et al prepared a porous Fe_3O_4-HAp composite using a hydrothermal method. The composite holds 30% Fe_3O_4 in cages of rod-shaped HAp particles.[8] Fe_3O_4 nanoparticles are prepared by a coprecipitation method, and a horizontal tumbling ball mill is used to mechanochemically synthesize submicron-sized HAp particles. According to Iwasaki et al[9] this process promotes the dispersion of Fe_3O_4 nanoparticles in the HAp matrix. The magnetic Fe_3O_4 particles are coated with HAp by spray-drying. Donadel et al found that the spray-drying technique is an efficient and inexpensive method for creating spherical particles with a core/shell structure.[10] Tampieri et al prepared iron-doped HAp endowed with superparamagnetic properties for hyperthermic application.[11]

These composites can be synthesized conventionally by mixing HAp nanopowder with Fe_3O_4 nanoparticles that are prepared separately. In this work, Fe_3O_4 nanoparticles were prepared by alkaline coprecipitation of ferric and ferrous chloride in aqueous solution. Nanocrystalline HAp was prepared using an optimized sol-gel method. Dry (zirconia ball) milling was used to blend the Fe_3O_4-HAp (0.70 w/w) nanoparticles. The Fe_3O_4-HAp nanoparticles and their composite were analyzed by Fourier transform infrared spectroscopy, diffuse reflectance spectroscopy, scanning electron microscopy, thermogravimetric analysis, differential scanning calorimetry, vibrating sample magnetometry, and cytotoxicity tests. The method proposed in this paper is easy and cost-effective for preparing these nanocomposites. The synthesis and characterization of this biocompatible magnetic biomaterial is explained in detail, and the nanostructured Fe_3O_4-HAp composite is ideal for bone cancer therapy.

Materials and methods
Synthesis of iron oxide nanoparticles
Fe_3O_4 magnetic nanoparticles were synthesized by the alkaline coprecipitation method. The molar ratio of Fe^{3+}:Fe^{2+} chloride was maintained at 2:1. The prepared magnetite was black in color and the pH was maintained between 9 and 14.[12] The overall reaction is written as:

$$Fe^{2+} + 2Fe^{3+} + 8OH^- \rightarrow Fe_3O_4 + 4H_2O \qquad (1)$$
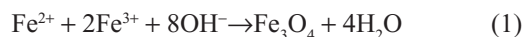
Synthesis of HAp nanoparticles
The HAp nanoparticles were prepared by the wet chemical route method. First, 0.25 M phosphoric acid was prepared in distilled water. Ammonia (NH_3) was added to this solution, with stirring to maintain the pH at 10. Next, a 1 M calcium nitrate tetrahydrate solution was prepared by dissolving in double-distilled water, which was then added slowly to the above phosphoric acid-ammonia solution. The solution was stirred vigorously for 1 hour and allowed to age at room temperature for 24 hours. The gel obtained after aging was dried at 80°C for 48 hours in a dry oven. The resulting mixture were washed repeatedly using distilled water. After washing, the powder was sintered for 2 hours at a temperature of 900°C.

Synthesis of Fe_3O_4-HAp nanocomposites
The Fe_3O_4-HAp nanocomposites were prepared using a wet-type ball mill (Figure 1A). The ratio of HAp to Fe_3O_4 nanoparticles was 1.5:1 (w/w). Ball milling was carried out for 5 hours using a zirconia bowl and ball at 300 rpm, with a ball to sample powder ratio of 10:1 (w/w).

Characterization
Fourier transform infrared spectra were taken using an 8400S spectrophotometer (Shimadzu, Tokyo, Japan). KBr pellets were used, and the spectra were recorded in aqueous medium.

The morphology of the Fe_3O_4-HAp nanostructures was observed using a scanning electron microscope (ICON, Quanta 200 Mark II Environmental scanning electron microscope) with an acceleration voltage of 0.2–30 kV.

The thermal properties of the prepared nanocomposites were investigated using a thermal analyzer (STA 449 F3 Jupiter, Netzsch Gerätebau GmbH, Selb, Germany) along with thermogravimetry and differential scanning calorimetry in the temperature range of 28°C–1,100°C at a heating rate of 20°C per minute in a dry air atmosphere. Al_2O_3 was used as the reference material.

Diffuse reflectance spectroscopy was performed using a Specord 210 Plus (Analytik Jena, The Woodlands, TX, USA) between 190 and 1,100 nm at room temperature.

The superparamagnetic properties of the Fe_3O_4-HAp nanocomposites were studied using a 7410 vibrating sample magnetometer (Lake Shore, Westerville, OH, USA), in atmospheric air at room temperature.

The cytotoxic effects of the Fe_3O_4-HAp nanocomposites were evaluated using MG63 cells. The MTT assay was performed according to the procedure shown in Figure 2. The formazan was dissolved in dimethyl sulfoxide and the absorbance of the solution was quantified at 510 nm.
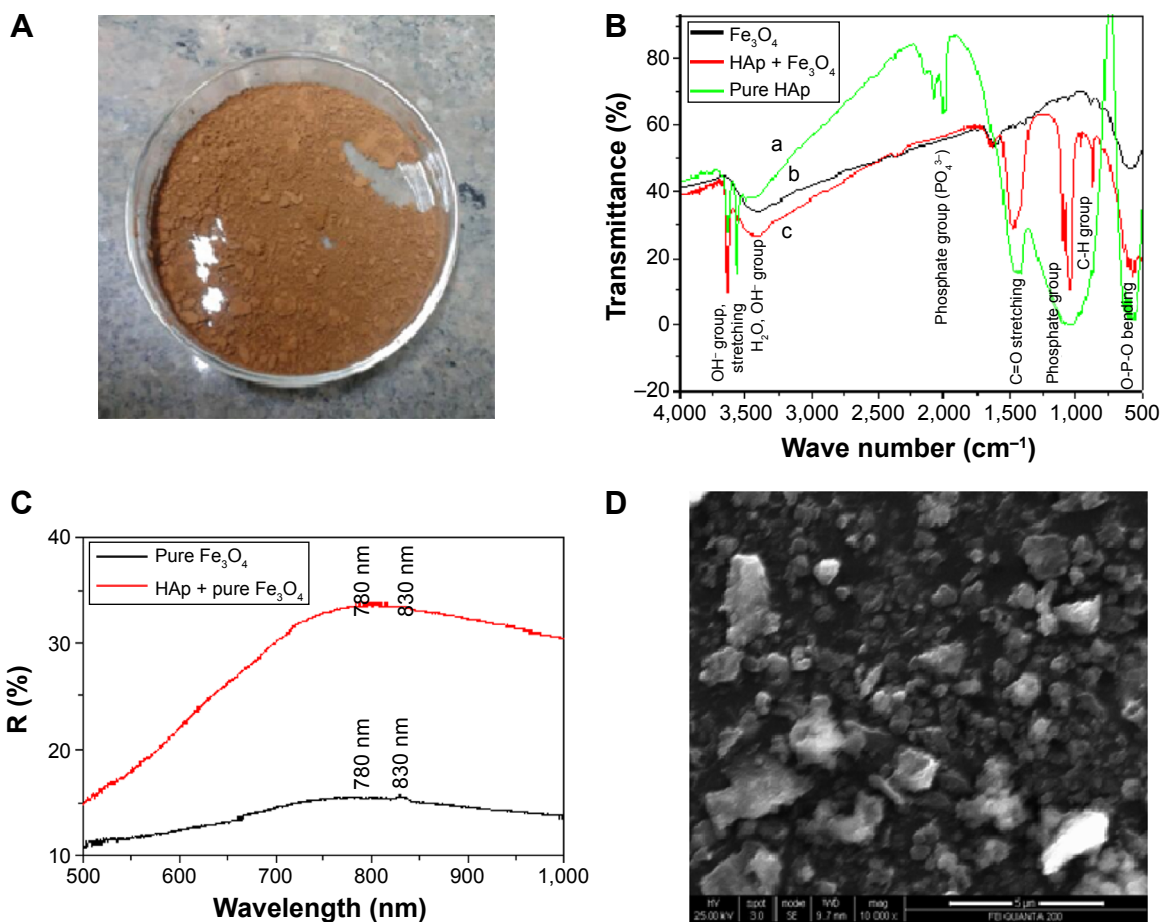
Figure 1 (**A**) Fe_3O_4-HAp nanoparticles in powder form. (**B**) Fourier transform infrared spectra of HAp, Fe_3O_4, and Fe_3O_4-HAp nanoparticles. (**C**) Diffuse reflectance spectra of magnetite and the composite. (**D**) Scanning electron micrograph of Fe_3O_4-HAp nanoparticles.
Abbreviations: Fe_3O_4, iron oxide; HAp, hydroxyapatite.

Results and discussion
Fourier transform infrared spectroscopy
The Fourier transform infrared spectral assignments for pure Fe_3O_4, HAp, and the Fe_3O_4-HAp nanoparticles are shown in Figure 1B and tabulated in Table 1. From these data, the functional groups of prepared samples confirms the presence of pure Fe_3O_4 and pure HAp. IN Fe_3O_4-HAp nanoparticles, a slight variation in spectral assignments confirms the close interaction between Fe_3O_4 and HAp.

Diffuse reflectance spectroscopy
Diffuse reflectance spectroscopy provides the electron transition of pure and mixed samples. Figure 1C represents the diffuse reflectance spectra for pure Fe_3O_4 and Fe_3O_4-HAp. Pure Fe_3O_4 shows a wavelength ($^4T_1$) transition in the range of 780–830 nm and an electron pair transition of 510 nm. This shows a higher position of the ligand-to-metal charge transfer transition and pair transition band of red Fe_3O_4.

Scanning electron microscopy
The micromorphology and texture of the Fe_3O_4-HAp nanocomposites are shown in Figure 1D. This scanning electron microscopic image shows that pure Fe_3O_4 has an irregular approximately spherical-like morphology with an average particle size in the range of 50–70 nm and that HAp has a particle size in the range of 30–40 nm. The aggregated Fe_3O_4-HAp clusters have a size range of 100–350 nm and both phases distributed uniformly, as shown in Figure 1D. The characteristic dark and light gray represents the Fe_3O_4 and HAp, respectively.

Thermogravimetric analysis
The Fe_3O_4-HAp nanoparticles were studied by thermogravimetric analysis in a nitrogen atmosphere at a heating rate of 20°C per minute. Figure 3 shows the thermogravimetric analysis curves, depicting the variations in residual mass of the samples with increasing temperature. The absolute weight loss from
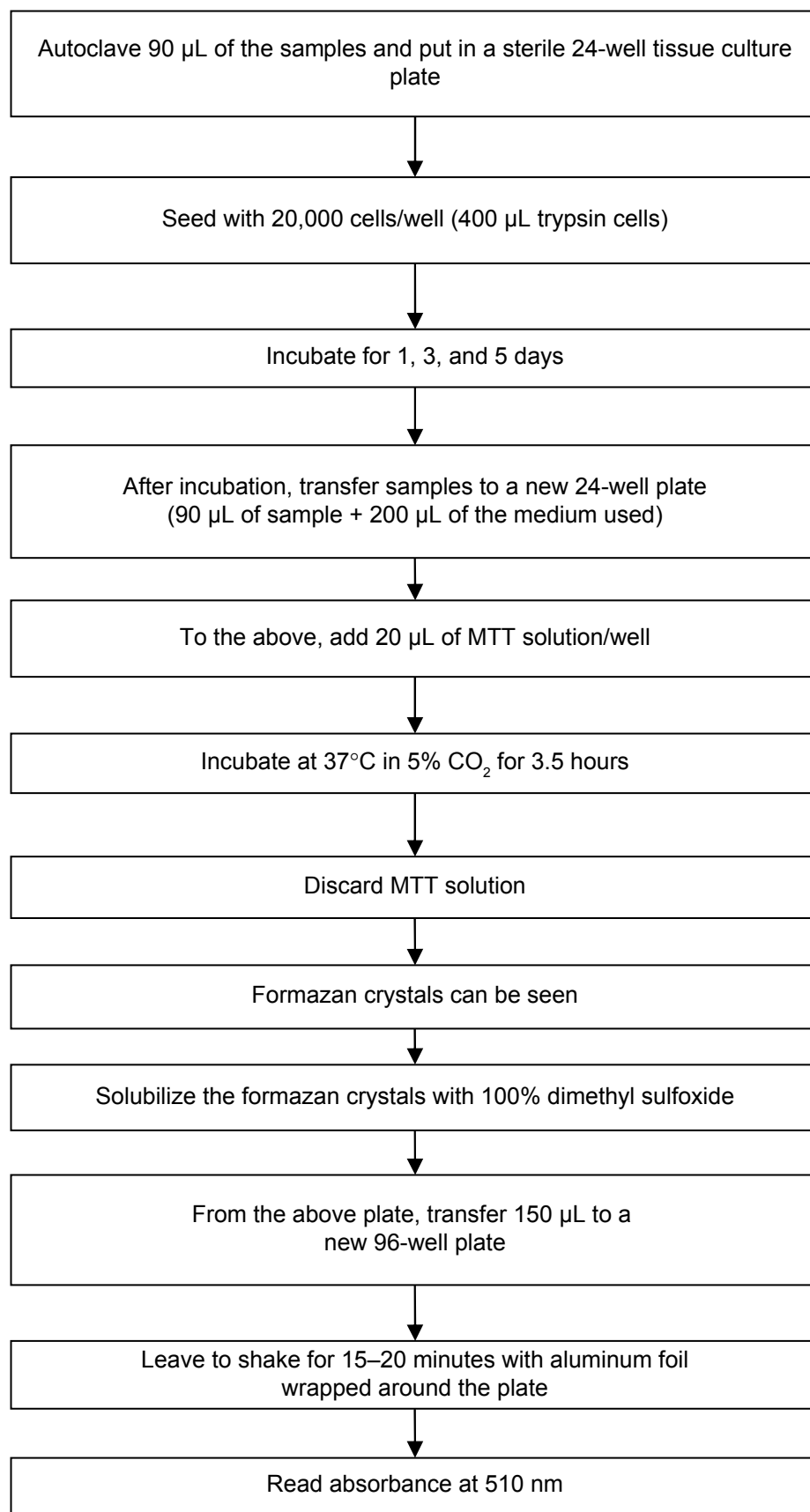
Autoclave 90 μL of the samples and put in a sterile 24-well tissue culture plate

↓

Seed with 20,000 cells/well (400 μL trypsin cells)

↓

Incubate for 1, 3, and 5 days

↓

After incubation, transfer samples to a new 24-well plate
(90 μL of sample + 200 μL of the medium used)

↓

To the above, add 20 μL of MTT solution/well

↓

Incubate at 37°C in 5% CO_2 for 3.5 hours

↓

Discard MTT solution

↓

Formazan crystals can be seen

↓

Solubilize the formazan crystals with 100% dimethyl sulfoxide

↓

From the above plate, transfer 150 μL to a
new 96-well plate

↓

Leave to shake for 15–20 minutes with aluminum foil
wrapped around the plate

↓

Read absorbance at 510 nm

Figure 2 Flow chart showing the MTT assay procedure.

Table 1 Fourier transform infrared spectral assignments of pure Fe_3O_4, HAp, and Fe_3O_4-HAp nanoparticles

S No	Wave number (cm^{-1})			Spectral assignments
	Fe_3O_4	HAp	Fe_3O_4-HAp	
1	–	3,639	3,639	OH$^-$ group, CaO
2	–	3,561	3,570	Stretching mode of OH$^-$ group
3	3,420	–	3,420	H_2O, OH$^-$ group
4	–	2,080	–	Phosphate group (PO_4^{3-})/absorbed CO_3^{2-}
5	–	2,003	–	Phosphate group (PO_4^{3-})/absorbed CO_3^{2-}
6	–	–	1,638	O-H in-plane bending
7	1,625	–	–	(H-O-H) adsorbed water
8	–	1,473	1,473	CO_3^{2-}
9	1,383	–	–	N-O nitro compounds
10	1,151	–	–	C-O
11	–	–	1,091	Phosphate group (PO_4^{3-})
12	1,062	–	–	C-O
13	–	1,046	1,046	Phosphate group (PO_4^{3-})
14	–	–	960	Phosphate group (PO_4^{3-})
15	891	–	–	C-H
16	–	–	875	C-H
17	797	–	–	C-H
18	–	–	629	C-Cl
19	–	–	601	O-P-O bending
20	588	–	–	Fe-O-Fe bond (Fe ions in tetrahedral and octahedral site)
21	–	566	566	O-P-O bending

Abbreviations: Fe_3O_4, iron oxide; HAp, hydroxyapatite.

the uncoated Fe_3O_4 is nearly 17% for the whole temperature range due to removal of adsorbed physical and chemical water. Another 5% weight loss was seen from 160°C to 300°C, and this was associated with decomposition of residual chemical compounds. No significant weight loss was observed at higher temperatures. Thermogravimetric analysis of the Fe_3O_4-HAp powder showed weight loss up to a temperature of 800°C and thereafter weight remained constant.

The first stage of weight loss is between 90°C and 390°C, which corresponds to dehydration of the precipitating complex and loss of physically adsorbed water molecules from the HAp powder. The weight loss in this region is 10%.
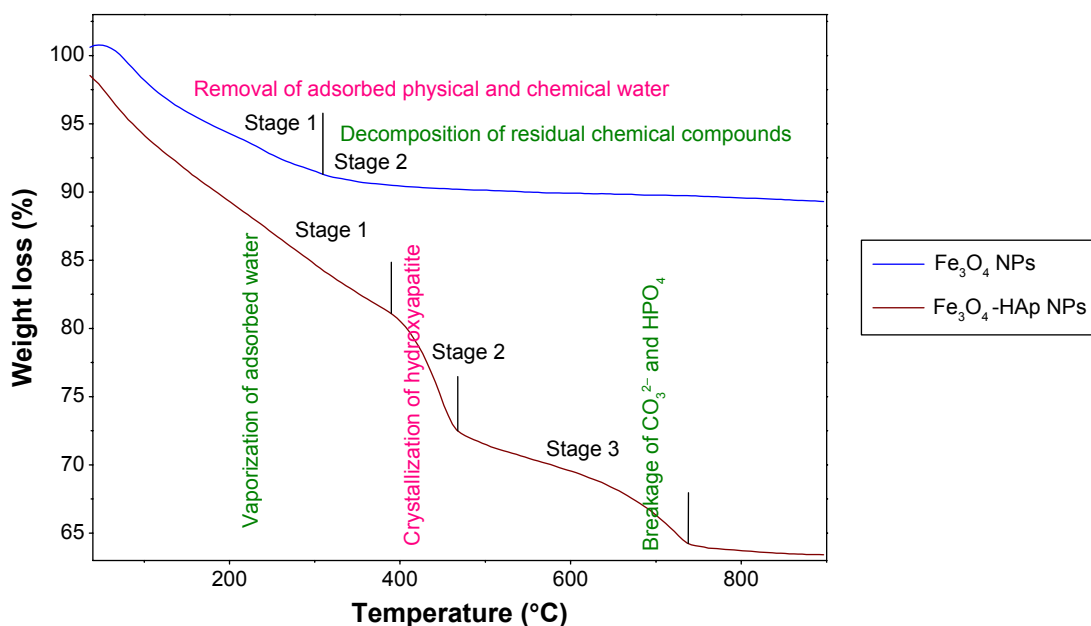
Figure 3 Weight loss from the Fe_3O_4-HAp nanoparticles.
Abbreviations: Fe_3O_4, iron oxide; HAp, hydroxyapatite; NPs, nanoparticles.

Stage 1 corresponds to vaporization of adsorbed water on the surface of HAp, stage 2 is due to vaporization of the water and crystallization of HAp, and stage 3 is probably due to breakage of CO_3^{2-} and HPO_4 in HAp.

Differential scanning calorimetry

The differential scanning calorimetry analysis of Fe_3O_4 and the nanocomposite is shown in Figure 4. The pure Fe_3O_4 shows a strong endothermic peak approximately 100°C. This is due to removal of the solvent molecule (H_2O). A slight endothermic transition approximately 620°C indicates crystallization of the magnetite phase. The differential scanning calorimetry results for the Fe_3O_4-HAp nanocomposite show a strong endothermic peak located in the range of 90°C–110°C. Two exothermic peaks were identified at 470°C and 720°C. The first one could be due to crystallization of the powder, given that this temperature range allows strong interaction between Fe_3O_4 and HAp molecules. The second one corresponds to the rearrangement of the CO_3^{2-} and HPO_4^- groups present in HAp. This is in good agreement with the thermogravimetric analysis.

Vibrating sample magnetometry

The magnetic hysteresis loops for the Fe_3O_4 nanoparticles and the Fe_3O_4-HAp nanocomposites is shown in Figure 5. These materials exhibited strong magnetic behavior, with saturation magnetization of 20.639 and 7.34 emu/g and coercivity of 4.1747 and 5.1233 G, respectively, at 300 K. The magnetic properties are tabulated in Table 2. The

saturation magnetization of pure Fe_3O_4 is lower than the value reported in the literature (92 emu/g).[13] The samples show typical superparamagnetic behavior, with near zero coercivity and remanent magnetization, whereas pure HAp does not have any hysteresis loop. It is also clear from vibrating sample magnetometry that the magnetite particle in the composite structure is well within the single domain particle range and exhibits superparamagnetism. The magnetization value of the composites was lower than that of the pure Fe_3O_4 nanoparticles. The decreased saturation magnetization could be due to interaction between the iron core and the HAp shell, which decreases the magnetic moment.[14,15]

Cytotoxicity testing

In vitro cytotoxicity assays are the primary biocompatibility screening tests for a wide variety of materials used in the medical field. The MTT assay was done for the Fe_3O_4 and Fe_3O_4-HAp nanoparticles using MG63 (osteosarcoma) cells. Three concentrations (1, 3, and 5 mg/mL) of the Fe_3O_4 nanoparticles and the Fe_3O_4-HAp nanocomposites were tested. The experiments were performed in triplicate. The mean values obtained are shown in Figure 6. The MTT assay procedure is explained in the flow chart given in Figure 2. The results show that the Fe_3O_4-HAp nanoparticles enabled better cell proliferation than the pure Fe_3O_4 at the concentrations tested.

Magnetic induction hyperthermia is a technique that can be used to destroy cancer cells via their hysteresis loss
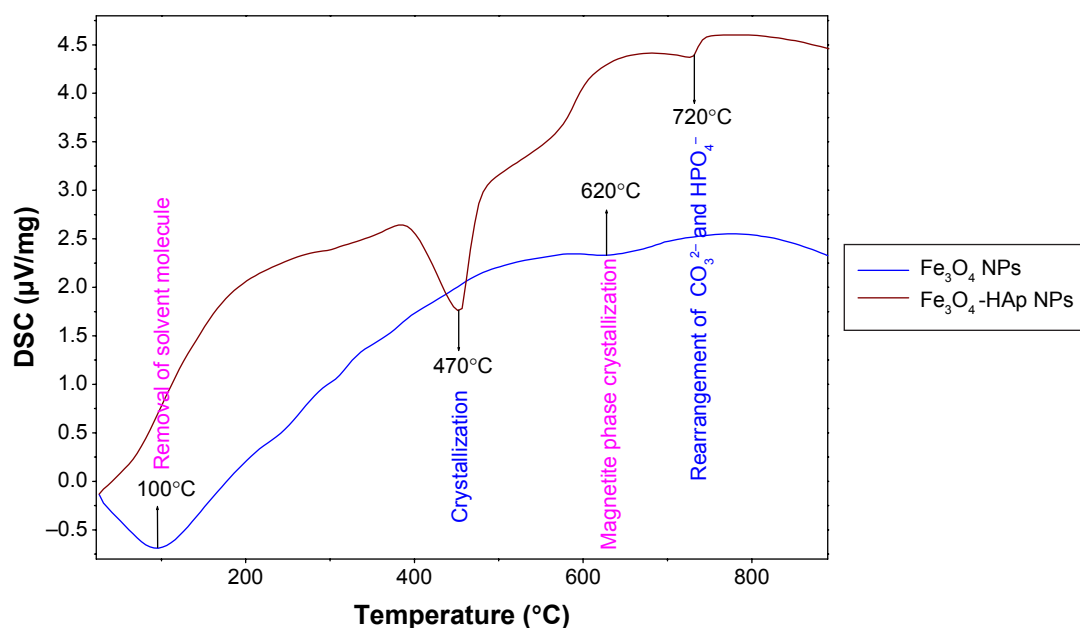
Figure 4 DSC analysis of Fe_3O_4-HAp nanoparticles.
Abbreviations: DSC, differential scanning calorimetry; Fe_3O_4, iron oxide; HAp, hydroxyapatite; NPs, nanoparticles.
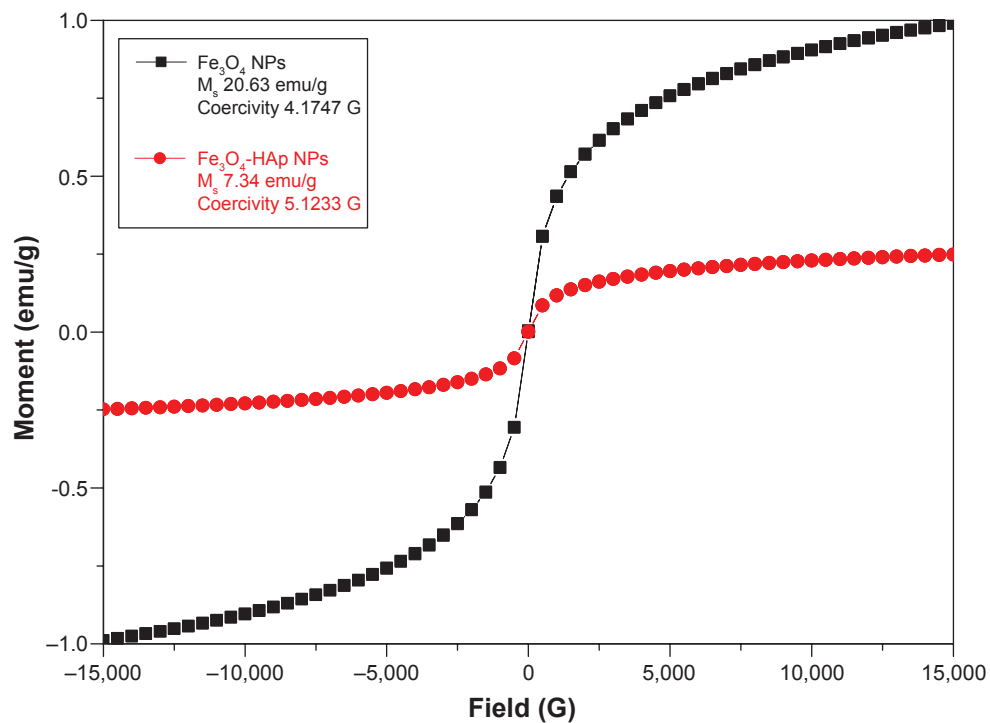
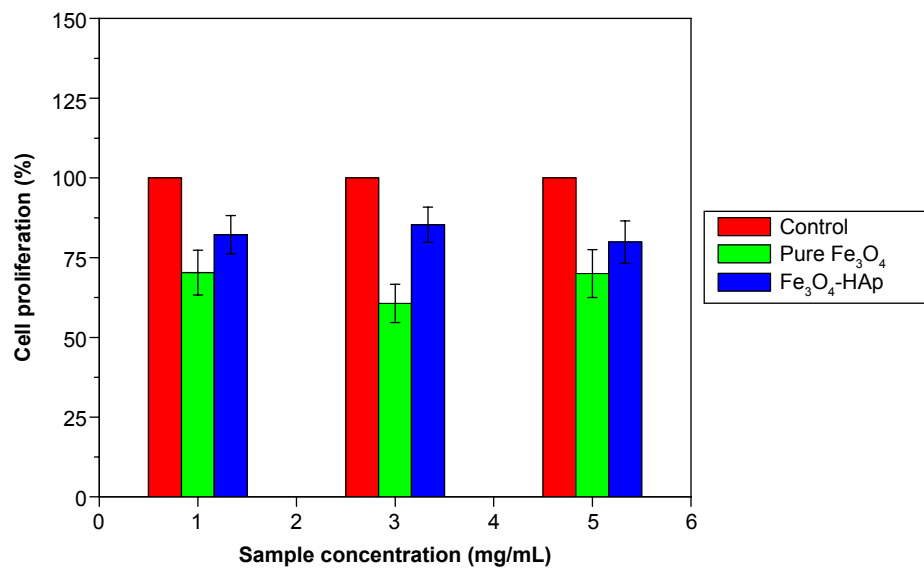**Figure 5** Magnetic hysteresis loops of pure Fe_3O_4 and Fe_3O_4-HAp nanoparticles.
Abbreviations: Fe_3O_4, iron oxide; HAp, hydroxyapatite; NPs, nanoparticles; M_s, saturation magnetization.

Table 2 Magnetic properties of Fe_3O_4 and Fe_3O_4-HAp nanoparticles

Sample	Coercivity (G)	Saturation magnetization (emu/g)	Remanent magnetization (G)
Fe_3O_4 nanoparticle	4.1747	20.639	0
Fe_3O_4-HAp nanocomposite	5.1233	7.34	0

Abbreviations: Fe_3O_4, iron oxide; HAp, hydroxyapatite.

Figure 6 Cytotoxicity test for pure Fe_3O_4 and Fe_3O_4-HAp nanoparticles.
Abbreviations: Fe_3O_4, iron oxide; HAp, hydroxyapatite.

when placed in an alternating magnetic field. The prepared nanocomposites have the capacity to generate heat in the presence of an alternating magnetic field. The temperature of the cancer cells is raised between 42°C and 46°C via the heat produced by our prepared composite materials. Although the heating efficiency of the prepared superparamagnetic Fe_3O_4-HAp nanocomposite is not demonstrated here, Hou et al[16] showed that a similar Fe_3O_4-HAp nanocomposite was capable of magnetically inducing effective thermal destruction of cancer cells in vivo.

Conclusion

In this work, pure Fe_3O_4 was prepared by alkaline coprecipitation and HAp nanoparticles were prepared using an optimized sol-gel method. Fe_3O_4-HAp (0.7 w/w) nanocomposites were developed by wet milling. The prepared Fe_3O_4-HAp nanoparticles and its composite were characterized and confirmed by scanning electron microscopy, Fourier transform infrared spectroscopy, and diffuse reflectance spectroscopy. Their superparamagnetic nature was confirmed by vibrating sample magnetometry, and their thermal stability was confirmed by thermogravimetric analysis and differential scanning calorimetry. This nanostructured Fe_3O_4-HAp composite would be ideal for use in bone cancer therapy.

Acknowledgments

Disclosure

The authors report no conflicts of interest in this work.

References

1. Jiang QL, Zheng SW, Hong RY, et al. Folic acid conjugated Fe_3O_4 magnetic nanoparticles for hyperthermia and MRI in vitro and in vivo. *Appl Surf Sci.* 2014;307:224–233.
2. Di Corato R, Espinosa A, Lartigue L, et al. Magnetic hyperthermia efficiency in the cellular environment for different nanoparticle designs. *Biomaterials.* 2014;35:6400–6411.
3. Pankhurst QA, Connolly J, Jones SK, Dobson J. Applications of magnetic nanoparticles in biomedicine. *J Phys D Appl Phys.* 2003;36: R167–R181.
4. Bear JC, Yu B, Blanco-Andujar C, et al. A low cost synthesis method for functionalised iron oxide nanoparticles for magnetic hyperthermia from readily available materials. *Faraday Discuss.* 2014;175:83–95.
5. Bonnemain B. Superparamagnetic agents in magnetic resonance imaging: physicochemical characteristics and clinical applications – a review. *J Drug Target.* 1998;6:167–174.
6. Singh RK, El-Fiqi AM, Patel KD, Kim HW. A novel preparation of magnetic hydroxyapatite nanotubes. *Mater Lett.* 2012;75:130–133.
7. Karunamoorthi R, Kumar GS, Prasad AI, Vatsa RK, Thamizhavel A, Girija EK. Fabrication of a novel biocompatible magnetic biomaterial with hyperthermia potential. *J Am Ceram Soc.* 2014;97:1115–1122.
8. Murakami S, Hosono T, Jeyadevan B, Kamitakahara M, Ioku K. Hydrothermal synthesis of magnetite/hydroxyapatite composite material for hyperthermia therapy for bone cancer. *J Am Ceram Soc.* 2008; 116:950–954.
9. Iwasaki T, Nakatsuka R, Murase K, Takata H, Nakamura H, Watano S. Simple and rapid synthesis of magnetite/hydroxyapatite composites for hyperthermia treatments via a mechanochemical route. *Int J Mol Sci.* 2013;14:9365–9378.
10. Donadel K, Felisberto MD, Laranjeira MC. Preparation and characterization of hydroxyapatite-coated iron oxide particles by spray-drying technique. *An Acad Bras Cienc.* 2009;81:179–186.
11. Tampieri A, D'Alessandro T, Sandri M, et al. Intrinsic magnetism and hyperthermia in bioactive Fe-doped hydroxyapatite. *Acta Biomater.* 2012;8:843–851.
12. Gupta AK, Gupta M. Synthesis and surface engineering of iron oxide nanoparticles for biomedical applications. *Biomaterials.* 2005;26: 3995–4021.
13. Bretcanu O, Spriano S, Brovarone C, Verne E. Synthesis and characterization of coprecipitation-derived ferromagnetic glass-ceramic. *J Mater Sci.* 2006;41:1029–1037.
14. Cheng J, Ni X, Zheng H, Li B, Zhang X, Zhan D. Preparation of Fe (core)/SiO_2 (shell) composite particles with improved oxidation resistance. *Mater Res Bull.* 2006;41:1424–1429.
15. Ramanujan RV, Yeow YY. Synthesis and characterization of polymer-coated metallic magnetic materials. *Mater Sci Eng C.* 2005;25:39–41.
16. Hou CH, Hou SM, Hsueh YS, Lin J, Wu HC, Lin FH. The in vivo performance of biomagnetic hydroxyapatite nanoparticles in cancer hyperthermia therapy. *Biomaterials.* 2009;30:3956–3960.